Projection of $\mathfrak{L}\bar{v}_0$ on the z axis indicates that

$$\frac{\partial}{\partial z}\left[\nabla_M^2 A - \frac{m^2}{r^2} A\right] = 0.$$

In consequence, $\nabla_M^2 A - (m^2/r^2)A$ has a constant value along a parallel to the z axis. This value must be zero, because

$$\nabla_M^2 A - \frac{m^2}{r^2} A = 0 \tag{52}$$

on c. It follows that (52) is valid over the whole area D. An application of Green's theorem shows that

$$\int\int_D \left\{\frac{m^2}{r^2} A^2 + |\operatorname{grad} A|^2\right\} r dr dz = 0$$

so that both A and $\bar{v}_0$ must vanish.

The self-adjoint character of $\mathfrak{L}$ (*i.e.*, $\langle \bar{c}, \mathfrak{L}\bar{d}\rangle = \langle \bar{d}, \mathfrak{L}\bar{c}\rangle$) can be quickly established by using a relation derived from the three-dimensional Green's theorem (32):

$$\int\int_D \left\{\overline{Q}\cdot\left(\nabla_M^2 \overline{P} - \frac{m^2}{r^2}\overline{P} + \frac{2mg}{r^2}\bar{u}_r\right) + h\left(\nabla_M^2 g - \frac{m^2+1}{r^2} g + \frac{2mc_r}{r^2}\right)\right.$$
$$+ \left(\operatorname{div}_M \overline{P} - \frac{mg}{r}\right)\cdot\left(\operatorname{div}_M \overline{Q} - \frac{mh}{r}\right) + \operatorname{curl}_M \overline{P}\cdot\operatorname{curl}_M \overline{Q}$$
$$\left.+\left[\operatorname{curl}_M (g\bar{u}_\phi) + \frac{m}{r}(\bar{u}_\phi \times \overline{P})\right]\cdot\left[\operatorname{curl}_M (h\bar{u}_\phi) + \frac{m}{r}(\bar{u}_\phi \times \overline{Q})\right]\right\} r dr dz$$
$$= \int_c \left\{(\bar{u}_n \times \overline{Q})\cdot\operatorname{curl}_M \overline{P} - \frac{hm}{r}(\bar{u}_n\cdot\overline{P}) - h\bar{u}_t\cdot\operatorname{curl}_M (g\bar{u}_\phi) + (\bar{u}_n\cdot\overline{Q})\left(\operatorname{div}_M \overline{P} - \frac{mg}{r}\right)\right\} r dc. \tag{53}$$

If we use this relation twice, setting $g = r/m \operatorname{div}_M \overline{P}$, $h = r/m \operatorname{div}_M \overline{Q}$ and subtracting, we obtain, since

$$\operatorname{div}_M\left[\nabla_M^2 \bar{c} - \frac{m^2\bar{c}}{r^2} + \frac{2}{r}\cdot\bar{u}_r \operatorname{div}_M \bar{c}\right]$$
$$= \frac{m}{r}\nabla_M^2\left(\frac{r \operatorname{div}_M \bar{c}}{m}\right) + \frac{2m^2}{r^3} c_r - \frac{m^2+1}{r^2}\operatorname{div}_M \bar{c}$$
$$= \nabla_M^2 (\operatorname{div}_M \bar{c}) - \frac{m^2}{r^2}\operatorname{div}_M \bar{c} + \frac{2m^2}{r^3} c_r + \frac{2}{r}\frac{\partial}{\partial r}(\operatorname{div}_M \bar{c}), \tag{54}$$

the relation,

$$\int\int_D \left[\overline{Q}\cdot\mathfrak{L}\overline{P} - \overline{P}\cdot\mathfrak{L}\overline{Q} + \frac{r^2}{m^2}\operatorname{div}_M \overline{Q} \operatorname{div}_M \mathfrak{L}\overline{P}\right.$$
$$\left. - \frac{r^2}{m^2}\operatorname{div}_M \overline{P} \operatorname{div}_M \mathfrak{L}\overline{Q}\right] r dr dz = 0. \tag{55}$$

The second member in (53) vanishes because of the boundary conditions. Eq. (55) is nothing but $\langle \bar{c}, \mathfrak{L}\bar{d}\rangle - \langle \bar{d}, \mathfrak{L}\bar{c}\rangle = 0$, the relation we set out to prove.

A Printed Circuit Balun for Use with Spiral Antennas*

R. BAWER† AND J. J. WOLFE†

Summary—A novel printed circuit balun is described which is particularly well suited to applications where space is at a premium. The design utilizes unshielded strip transmission line, but is readily adaptable to all of the common printed circuit transmission line techniques. When the balun is housed within the cavity of a spiral antenna, boresight error is virtually eliminated, ellipticity ratios of less than 2 db are maintained over an azimuth angle greater than $\pm 60°$, and the input standing-wave ratio is less than 2:1 over an octave frequency range. Experimental results are given and additional applications are described.

* Manuscript received by the PGMTT, October 16, 1959; revised manuscript received, November 23, 1959. The work reported in this paper was sponsored by the Airborne Instruments Lab., Div. of Cutler-Hammer, Inc., Melville, N. Y., P.O. No. 6468, under Air Force Contract No. AF33(600)-37929.

† Aero Geo Astro Corp., Alexandria, Va.

I. Introduction

A BALUN is a term used by antenna engineers to describe a device which transforms an unbalanced to a balanced transmission line. To the microwave engineer, the same device might be called a ratrace, magic tee, or more generally a hybrid. In lumped circuit applications, we also find a similar device used in conjunction with balanced mixers, phase detectors, and single-sideband modulators, to name a few. However, regardless of what the device is called, the operation will appear to be basically similar provided the analysis is made using a compatible frame of reference. One particularly powerful tool used at microwaves

involves the circuit symmetry; however, for the particular baluns to be described, this approach is somewhat mathematical in nature and tends to obscure the physical significance of the various parameters. On the other hand, the equivalent circuit representation clearly places in evidence the role of each element of the unit and provides the designer with a compact analytic expression for the input impedance.

There are numerous devices[1-5] which are suitable for transforming a balanced to an unbalanced transmission line over a wide frequency range. The balun to be described here is nothing more than a novel realization of a conventional type of balun which is particularly suited for use with spiral antennas or similar applications where space is at a premium.

Fig. 1 shows the schematic drawing and equivalent circuit of a coaxial balun proposed by Roberts.[1] Z_a and Z_b represent the characteristic impedance of the transmission lines a and b, respectively. Z_{ab} is the characteristic impedance of the balanced transmission line composed of the outer conductors of lines a and b.

From the equivalent circuit, the impedance looking into the terminals D–G can be directly written as

$$Z = -jZ_b \cot \theta_b + \frac{jRZ_{ab} \tan \theta_{ab}}{R + jZ_{ab} \tan \theta_{ab}}. \quad (1)$$

On letting $\theta_b = \theta_{ab} = \theta$ and rationalizing, the following expression is obtained

$$Z = \frac{RZ_{ab}^2 + j \cot \theta [R^2(Z_{ab} - Z_b \cot^2 \theta) - Z_b Z_{ab}^2]}{Z_{ab}^2 + R^2 \cot^2 \theta}. \quad (2)$$

Two interesting cases have been treated in the literature. Roberts[1] imposes the conditions that $Z_b = Z_a$ and $Z_{ab} = R$. For this case,

$$Z = R \sin^2 \theta + j(\cot \theta)(R \sin^2 \theta - Z_a) \quad (3)$$

and the input impedance becomes perfectly matched at two widely-separated frequencies given by the solution of

$$\sin^2 \theta = Z_a/R. \quad (4)$$

These frequencies are symmetrically disposed about a center frequency corresponding to $\theta = 90°$.

Using essentially the same prototype balun, McLaughlin, *et al.*,[2] obtained a considerably greater bandwidth by minimizing the imaginary term in (2). Again, θ is chosen to be 90° at midband, Z_b is chosen according to

$$Z_b = R^2/Z_{ab}, \quad (5)$$

and Z_{ab} is made as large as possible.

In order to compare the two approaches, the standing-wave ratio curves shown in Fig. 2 were calculated for the case of a balun transforming a 50-ohm unbalanced load to a 70-ohm balanced load. The improvement of the more flexible form (*i.e.*, $Z_b = R^2/Z_{ab}$) is obvious. The advantage is somewhat offset by the increased complexity of the coaxial realization; however, this objec-

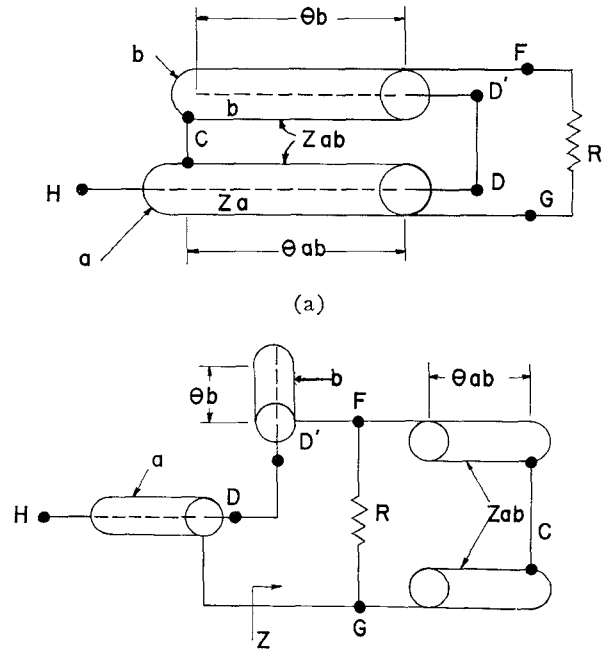

Fig. 1—Wide-band balun, from Roberts.[1] (a) Schematic drawing. (b) Equivalent circuit.

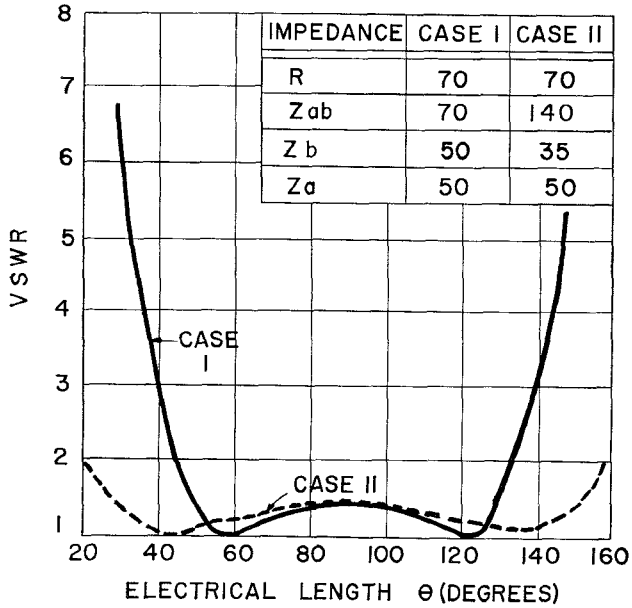

Fig. 2—Theoretical VSWR vs electrical length for two different balun design criteria.

[1] W. K. Roberts, "A new wide-band balun," PROC. IRE, vol. 45, pp. 1628–1631; December, 1957.
[2] J. W. McLaughlin, D. A. Dunn, and R. W. Grow, "A wide-band balun," IRE TRANS. ON MICROWAVE THEORY AND TECHNIQUES, vol. MTT-6, pp. 314–316; July, 1958.
[3] Radio Res. Lab. Staff, "Very High Frequency Techniques," McGraw-Hill Book Co., Inc., New York, N. Y., pp. 85–91; 1957.
[4] E. G. Fubini and P. J. Sutro, "A wide-band transformer from an unbalanced to a balanced line," PROC. IRE, vol. 35, pp. 1153–1155; October, 1947.
[5] E. M. T. Jones and J. K. Shimizu, "A wide-band strip-line balun," IRE TRANS. ON MICROWAVE THEORY AND TECHNIQUES, vol. MTT-7, pp. 128–134; January, 1959.

tion is no longer valid for the printed circuit balun.

It is important to note that, in both of the cases illustrated, the balun provides no impedance transformation at the center frequency. This fact is particularly significant in all applications in which the load impedance is considerably different than 50 ohms. A low standing-wave ratio can then be obtained only by the use of an independent impedance transformer.

The need for an impedance transformer in a small diameter coaxial line again suggests the use of printed circuit techniques; in this case, to alleviate the severe mechanical problems and high cost which might otherwise be incurred. Still another incentive stems from an assumption inherent in the equivalent circuit representation of the balun. In this analysis, it was tacitly assumed that the line length D–D' is small compared to the operating wavelength. The simultaneous requirements that Z_{ab} be large and the length D–D' be small, are obviously in conflict; moreover, this length becomes prohibitively long at frequencies greater than approximately 2000 mc.

To circumvent this difficulty, one can introduce right-angle bends in the coaxial lines a and b, and thereby reduce length D–D' to an arbitrarily small value. It is this coaxial structure that served as the prototype for the printed circuit balun.

II. Printed Circuit Balun

Fig. 3 illustrates the construction of the printed circuit balun. Note that the coaxial line of Fig. 1 has been replaced by unshielded strip transmission line and that the corresponding balanced transmission line now consists of the two ground planes.

For a given load and generator impedance, (2), (4), or (5) can be used to calculate the necessary parameter values. If, however, the mismatch corresponding to the ratio of load-to-generator impedance is greater than can be tolerated, an independent transforming section must be used. This can easily be accomplished by tapering the input transmission line.

The remaining steps of the design involve translating the calculated impedances and line lengths into actual physical dimensions of the printed line. At this point, it is important to consider any and all constraints which must be imposed on the balun. These constraints may be clearly defined, or may be contained within a broader specification, as in the case of the antenna assembly described in the next section.

With reference to Fig. 3, it is seen that two types of transmission line are involved. The first is the conventional unshielded strip transmission line consisting of a thin conductor over a ground plane; namely, lines a and b. The second type consists of a balanced transmission line made up of two flat, thin conductors of characteristic impedance Z_{ab} and length θ_{ab}. The simpler case will be discussed first.

The characteristic impedance and phase velocity of unshielded strip transmission line has been the subject of numerous articles.[6,7] The important point to remember is that virtually all of the field is confined within a region of about three conductor widths. Consequently, if the ground plane width is taken equal to or greater than three times the conductor width ($B>3b$), the resulting transmission line is, for all practical purposes, nonradiating. As this criterion is violated (say $b<B<3b$), the configuration takes on the appearance of a balanced transmission line and care must be exercised to minimize radiation caused by the unbalanced-to-balanced junction.

For reference purposes, approximate dimensions of unshielded strip transmission line for typical characteristic impedances are given in Table I. The reader is directed to the references for more complete data.

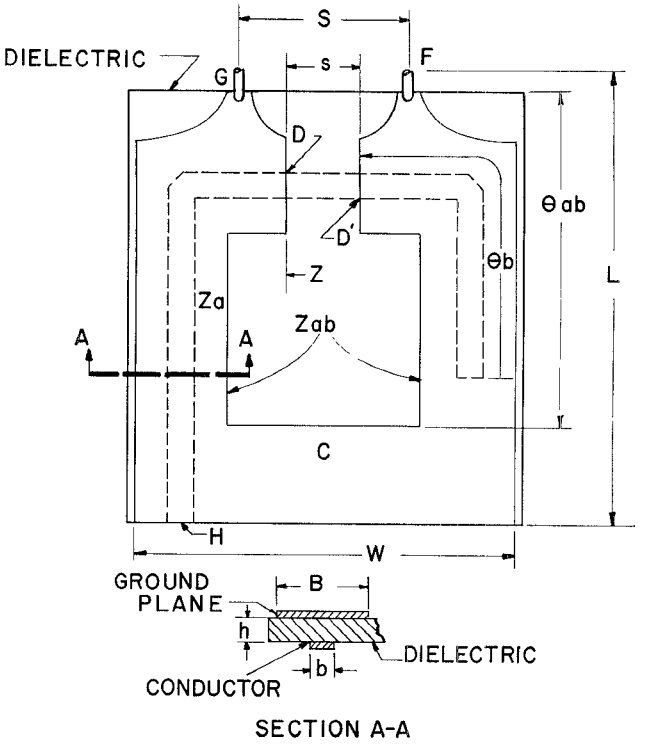

Fig. 3—Illustration of the construction of a printed circuit balun.

TABLE I

Characteristic Impedance of Unshielded Strip Transmission Line

($W>b$, $t=0$)

b/h	Material G-10 Z_0 (ohms)	Material GB-112 Z_0 (ohms)
0.75	90	125
1.0	80	112
1.5	65	89
2.0	53	74
2.5	46	64
3.0	41	55
4.0	33	46

[6] M. Arditi, "Characteristics of microstrip for microwave wiring," IRE Trans. on Microwave Theory and Techniques, vol. MTT-3, pp. 31–56; March, 1955.

[7] F. Assadourian and E. Rimai, "Simplified theory of microstrip transmission systems," Proc. IRE, vol. 40, pp. 1651–1657; December, 1952.

The physical length of the open-circuited transmission line (θ_b) depends upon the phase velocity in the printed circuit line. For the case of a homogeneous dielectric surrounding the lines, this phase velocity is given by

$$v = c/\sqrt{\epsilon} \tag{6}$$

where c is the velocity of light in free space and ϵ is the relative dielectric constant of the medium. Since the region between the conductor and the ground plane is filled with a dielectric while the remaining cross section is air, the problem becomes quite complex and one generally resorts to empirical techniques to establish the phase velocity. The velocity decreases as the width of the conductor increases and asymptotically approaches the velocity which would be obtained if the line were completely immersed in the dielectric.

In practice, the range of the ratio of conductor width to spacing above the ground plane is $1 < (b/h) < 5$. Over this range the phase velocity varies by about 10 per cent, which is well within the accuracy required for the balun design. Therefore, one may elect to use an average phase velocity (or average effective dielectric constant) instead of making the series of measurements necessary to describe the actual behavior. To this end, an approximate average effective dielectric constant can be taken as

$$\epsilon_e = 0.75\epsilon, \tag{7}$$

where ϵ is the dielectric constant of the base material. Eq. (6) can then be used for the initial calculation of θ_b, and the final length may easily be obtained by judicious trimming of the line length.

The impedance Z_{ab} and its corresponding phase velocity θ_{ab} present a more difficult problem. Short of actually attempting a solution to the problem using conformal mapping techniques, there appears to be no simple way to calculate or estimate the impedance of this configuration using available data. To further compound the problem, it may be recalled that the derivation of (1) was based on the assumption of a uniform balanced transmission line. The correct expression for the impedance Z of Fig. 3 must take into account not only the change in conductor spacing, but also the shape, length, and spacing of the terminals G–F. This is clearly no small undertaking.

In short, an analytic or approximate expression for the value of Z_{ab} is very desirable. Fortunately, the absence of this information has not proved detrimental, as attested to by the experimental results discussed in the next section. The redeeming feature can be attributed to the design requirement that Z_{ab} be as large as possible.

Nevertheless, some idea of the order of magnitude of Z_{ab} would be useful. To this end, measurements were taken over the range of strip widths and spacings which might be encountered in practice. The data were taken with a Boonton type 190 Q meter, using conventional lumped element measurement techniques to obtain the inductance and capacitance of each configuration. The characteristic impedance was then calculated from the relation

$$Z_{ab} = \sqrt{L/C} \text{ ohms}. \tag{8}$$

The phase velocity does not significantly depart from the free space value, a fact which is to be expected in light of the line configuration. The results are given in Table II and should be sufficiently accurate for most balun designs.

TABLE II

CHARACTERISTIC IMPEDANCE OF PRINTED BALANCED TRANSMISSION LINE

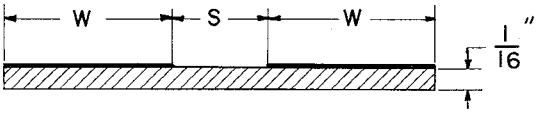

W/S	Z_0 (ohms)
2	220
4	185
6	170
8	160
10	155

III. Application to Spiral Antennas

The balun described here was developed to meet the need for a wide-band, compact device to feed a dual-arm spiral antenna from an unbalanced coaxial transmission line. It should be noted in passing that the printed circuit realization is not limited to this particular application, but is readily adaptable to a wide variety of uses. The printed circuit balun for spiral antennas represents one of the most stringent applications of this technique and, as such, clearly illustrates its extreme versatility.

At the onset of the development program, it was decided that the balun should be housed within the antenna structure. This necessarily imposed certain constraints on the physical size of the balun. In order to obtain a better insight into these constraints, a brief review of the operation of spiral antennas is given. The discussion is limited to those aspects which affect the balun design, and vice versa.

The spiral antenna[8] is one of a class of so-called "frequency independent" antennas which are completely described by angles except for diameter. Physically, the antenna is a two-dimensional structure which is fabricated by photo-etching the geometric configuration on copper-clad laminate. Of the wide variety of shapes possible, only three have received wide attention: the

[8] The spiral antenna was developed by W. E. Turner at Wright Air Dev. Center, Dayton, Ohio, in 1954. Since that time, most of the spiral antenna discussions have appeared as classified documents. A good unclassified reference is J. A. Kaiser, "Spiral antennas applied to scanning arrays," *Electronic Scanning Symp.*, Air Force Cambridge Res. Center, Bedford, Mass.; April, 1958. See also R. Bawer and J. J. Wolfe, "The Spiral Antenna," presented at 1960 IRE International Convention, New York, N. Y.; March 21–24, 1960. To be published in the 1960 IRE INTERNATIONAL CONVENTION RECORD.

logarithmic or equiangular spiral, the Archimedean spiral, and the rectangular counterpart of the Archimedean spiral. The printed antenna may be of the single or two-conductor configuration, the latter being preferable at frequencies below about 5000 mc. Functionally, the antenna radiates a bidirectional circularly polarized beam normal to the plane of the printed element when fed from a balanced two-wire transmission line. In most applications, the spiral antenna is flush-mounted (*e.g.*, in the skin of an aircraft), so that the bidirectional characteristics are undesirable; unidirectional patterns may be obtained by mounting the spiral at the mouth of a cylindrical cavity as shown in Fig. 4.

The gain of the cavity-backed spiral antenna follows the behavior one would expect from a dipole over a ground plane, being a maximum when the cavity depth is about $\frac{1}{4}\lambda$ and dropping off quite rapidly for depths less than the $\frac{1}{8}\lambda$ and greater than $\frac{3}{8}\lambda$. Since it is desirable to house the balun within the cavity, the length of the structure must be less than one-eighth of the free-space wavelength for maximum bandwidth. This requirement is based on the assumption that the balun will be mounted at right angles to the plane of the printed spiral as shown in the figure.

The allowable width of the balun is related to the radiating mechanism of the antenna. Although there is no rigorous theory to explain the radiation from spirals, the "Band Theory" quite adequately describes the phenomenon and is generally accepted by workers in the field. According to this theory, radiation from a tightly-wound spiral will occur from a band with mean diameter equal to λ/π. Therefore, the width of the balun structure in the vicinity of the spiral terminals should be considerably less than this diameter. If this criterion is violated, obscuration of the spiral occurs and the axial ratio of the antenna is severely affected. In fact, axial ratio measurements at the higher frequencies afford an excellent means for checking this criterion. Experimental data have indicated that satisfactory operation will result if the width of the balun in the vicinity of the antenna terminals is less than about $\lambda/8$.

In review, there are constraints which are imposed on the balun size by virtue of its use with a spiral antenna and the manner in which the balun is mounted in the antenna cavity. For the configuration shown in Fig. 4, the criteria $L \leq \frac{1}{8}(\lambda)$ maximum and $W \leq \frac{1}{8}(\lambda)$ minimum prove to be a useful rule of thumb. The dimension S, the spacing between the output terminals of Fig. 3, is made as small as practical and compatible with the input terminal spacing of the spiral antenna.

Finally, it seems reasonable to evaluate any balun in terms of its behavior under actual operating conditions; namely, when driven from a prescribed generator and terminated in prescribed load. Thus, the final evaluation of the printed balun feed for the spiral antenna should be based on the characteristics of the entire antenna structure. Typical specification for spiral antennas of the type considered are:

Frequency range—1 octave,
Axial ratio—3 db maximum,
VSWR—2:1 maximum,
Beam squint—$<5°$.

In the following section, some experimental results are discussed. The data are limited to the antenna configuration shown in Fig. 4 in which the balun is contained within the cavity and mounted at right angles to the plane of the spiral. Several alternate balun configurations and additional applications of the printed circuit balun are given in Section V.

IV. Experimental Results

A series of printed circuit baluns were developed to operate with cavity-backed spiral antennas over the frequency range of 104 mc through 4200 mc. The initial design effort was concentrated on the *S*-band unit, since this case represented the most severe situation from the point of size and, consequently, the most severe test of the validity of the approximations.

Fig. 5 illustrates the final form of the balun feed which was designed to operate with a 3-inch diameter, dual-arm, Archimedean spiral antenna. The balun was photo-etched on 1/32 inch thick, 2-ounce copper-clad epoxy fiberglass (G-10) and is approximately 1 inch long by $\frac{3}{4}$ inch wide.

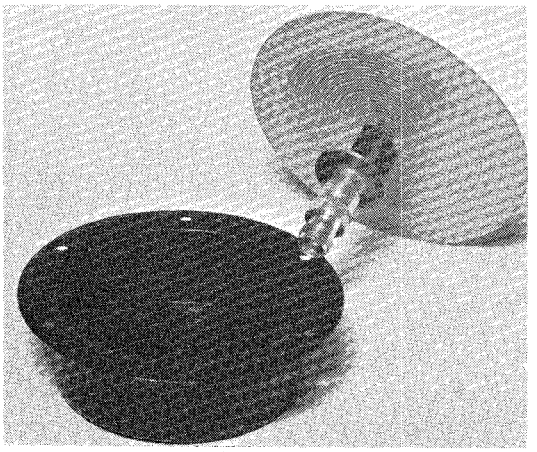

Fig. 4—An exploded view of a spiral antenna assembly.

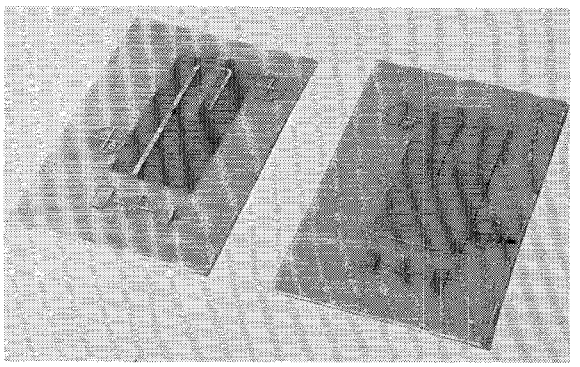

Fig. 5—Photograph of the final balun feed for an *S*-band spiral antenna.

Attention is specifically called to the following points:

1) The impedance of the spiral antenna was estimated to be in excess of 100 ohms; consequently, the input conductor was tapered to provide a characteristic impedance of about 50 ohms at the balun input and an impedance of about 100 ohms at the center line of the balun. The line continues at this impedance to the open circuit.
2) At the upper end of the frequency band, obscuration of the spiral by the balun resulted in an increased axial ratio. This effect was virtually eliminated by the simple expedient of trimming the corners of the ground plane as shown in Fig. 4.
3) The final results were obtained by systematically varying a number of the parameters. The major change involved the length of the open-circuited line θ_b which was adjusted to give a VSWR curve that is roughly symmetrical about the center frequency. The characteristic impedance and length of the balanced line Z_{ab} and θ_{ab} were found to have only a second-order effect.

Data showing the frequency dependence of the input impedance and axial ratio of a printed circuit balun and an *S*-band spiral antenna are shown in Fig. 6. If we neglect antenna gain, the major factor which limits the band-width of the antenna assembly is the axial ratio. The deterioration of axial ratio can be attributed to the spiral diameter at the low end of the frequency band (not illustrated) and balun size at the high end of the band. The input impedance is, of course, adversely affected at these limits also, but to a lesser extent than the axial ratio.

Fig. 7 illustrates the type of radiation patterns which have been obtained. The data were taken for two orthogonal cuts on an automatic pattern recorder with the antenna immersed in microwave absorbing material to simulate free space operating conditions. Axial ratio data (Fig. 6) were obtained by recording the maximum variation in the power received from a test antenna located on axis ($\phi=\theta=0$ degrees) as the spiral antenna was rotated 360°; this corresponds to the maximum difference (in db) between E_θ and E_ϕ at the origin of Fig. 7 for all orientations of the spiral.

There are two important points which should be emphasized. The first relates to range of azimuth angles over which the ellipticity ratio (E_0/E_θ) remains comparable to the on-axis ratio. For the particular cases illustrated, the ellipticity ratio remains less than 1 db over an azimuth angle of greater than $\pm 60°$.

The second point relates to the symmetry of the patterns about the axis of the antenna; beam squint is negligible. This behavior should be compared to that obtained with more conventional feeds in which beam squint in the order of 10° to 15° is common.

The results of the *S*-band balun are typical of the data which have been taken on units designed to operate as low as 140 mc. The chief difference between these baluns and the *S*-band unit is the thickness of the copper-clad material; for mechanical reasons, the lower-frequency baluns were photo-etched on 1/16-inch material.

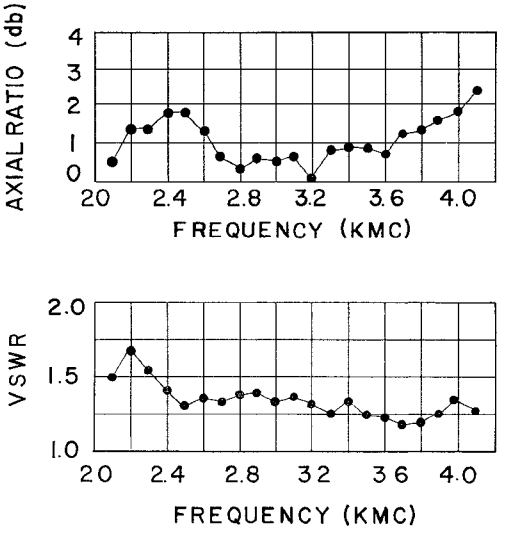

Fig. 6—Input impedance and axial ratio of a printed circuit balun and spiral antenna.

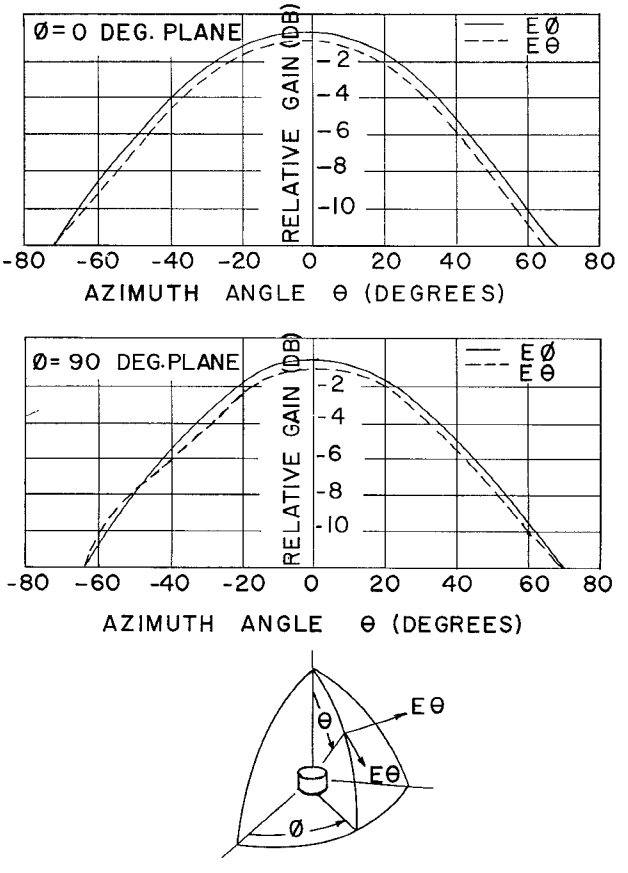

Fig. 7—Typical radiation patterns of an *S*-band spiral antenna fed from a printed circuit balun.

V. Conclusions

In the preceding discussion, a rather specialized application of a printed circuit balun was presented. The use of the balun with a cavity-backed spiral antenna, particularly when the balun is housed within the cavity, places severe limitations on the element size; it is expected that improved performance might be realized if these constraints were relaxed.

Nevertheless, this form factor does have some definite advantages which might not be immediately apparent. For example, by simply joining a second printed line at right angles to the balun (*i.e.*, normal to the printed line), the entire back plate of the cavity is made available for additional circuitry. In this manner, directional couplers, filters, etc., can easily be incorporated directly within the antenna structure with no space and negligible weight penalty.

An alternate configuration which appears to have some merit would involve mounting the balun parallel to the spiral and close to the cavity back plate. For this case, the size constraints can be significantly relaxed and the impedance transformer could now be placed in a printed balanced line connecting the balun output to the spiral input terminals. In other applications, it may be desirable to utilize a shielded configuration. The design described is equally applicable to all of the shielded strip transmission lines in common use.

In conclusion, it should be emphasized that the printed circuit balun is inherently capable of performance comparable to that of other wide-band baluns. With regard to basic design, nothing new is claimed. With regard to physical realization, it is believed that this printed circuit technique offers much in the way of ease of fabrication and miniaturization and, above all, a flexibility found in no other transmission line.

The *P-I-N* Modulator, an Electrically Controlled Attenuator for MM and Sub-MM Waves*

F. C. DE RONDE†, H. J. G. MEYER†, AND O. W. MEMELINK†

Summary—**The construction and performance of a millimeter wave modulator are described. The main part of the modulator consists of a *p-i-n* germanium structure inserted into a rectangular waveguide. A modulation depth of 11 db could be obtained at frequencies up to 5 kc, this modulation being caused for the greatest part by attenuation.**

I. Introduction

MICROWAVE modulators are used for various purposes, *e.g.* the formation of sidebands and particularly the increase of the sensitivity of measurements. In view of the great importance of having a modulator available, it is not surprising that various types of modulators are already in use to date.

The one most commonly employed is an absorption type modulator which makes use of a ferrite. Here the losses of the ferrite or the plane of its polarizing action are varied by a magnetic field. The necessity of using a magnetic field limits the modulating frequency to rather low values and the coils required make the device somewhat bulky.

Another type of modulator, also employing a magnetic field, was proposed by Gunn and Hogarth.[1] Here the number of free charge carriers in a semiconductor is varied by driving them either to a surface with a high or to a surface with a low value of the surface recombination velocity.

A modulator in which no use is made of a magnetic field is the so-called transparitor of Arthur, Gibson, and Granville.[2] Here the differential mobility of charge carriers in a semiconductor, and therefore its attenuation, is varied by the application of a strong electric field. An advantage of this arrangement is the possibility of employing very high modulation frequencies, the theoretical response time of the device being of the order of 10^{-12} seconds. A definite disadvantage for use under continuous wave conditions, however, is its great

* Manuscript received by the PGMTT, November 30, 1959; revised manuscript received, January 18, 1960.

† Philips Res. Labs., N. V. Philips' Gloeilampenfabrieken, Eindhoven, Netherlands.

[1] J. B. Gunn and C. A. Hogarth, "A novel microwave attenuator using germanium," *J. Appl. Phys.*, vol. 26, p. 353; March, 1955.

[2] J. B. Arthur, A. F. Gibson and J. W. Granville, "The effect of high electric fields on the absorption of germanium at microwave frequencies," *J. Electronics*, vol. 2, p. 145; September, 1956.